2020 IEEE International Conference on Robotics and Automation (ICRA)
31 May - 31 August, 2020. Paris, France

Proof-of-concept of a Pneumatic Ankle Foot Orthosis Powered by a Custom Compressor for Drop Foot Correction

Sangjoon J. Kim, Junghoon Park, Wonseok Shin, Dong Yeon Lee and Jung Kim, *Member, IEEE*

***Abstract*— Pneumatic transmission has several advantages in developing powered ankle foot orthosis (AFO) systems, such as the flexibility in placing pneumatic components for mass distribution and providing high back-drivability via simple valve control. However, pneumatic systems are generally tethered to large stationary air compressors that restrict them for being used as daily assistive devices. In this study, we improved a previously developed wearable (untethered) custom compressor that can be worn (1.5 kg) at the waist of the body and can generate adequate amount of pressurized air (maximum pressure of 1050 kPa and a flow rate of 15.1 mL/sec at 550 kPa) to power a unilateral active AFO used to assist the dorsiflexion (DF) motion of drop-foot patients. The finalized system can provide a maximum assistive torque of 10 Nm and induces an average 0.03±0.06 Nm resistive torque when free movement is provided. The system was tested for two unilateral drop-foot patients. The proposed system showed an average improvement of 13.6° of peak dorsiflexion angle during the swing phase of the gait cycle.**

I. Introduction

The number of people with age related disabilities and impairments have been steadily increasing worldwide [1], [2]. Among the wide range of realms of possible disabilities, gait related impairments have been of great interest as walking is a fundamental function of one's daily routine. As solutions to resolve such burdens, many forms of ankle foot orthoses (AFO) have been actively developed to provide functional independence to people with gait abnormality.

With the recent advances in actuator and sensors technology, a great amount of research efforts has been directed towards the development of powered AFOs. Powered AFOs are developed to provide assistive force/torque for plantarflexion (PF) or dorsiflexion (DF) of the ankle according to the gait phase to improve forward propulsion symmetry or assist foot clearance [3]–[8]. Many of these systems showed promising results in improving foot clearance and in reducing compensatory gait patterns (kinematic asymmetry) such as hip hiking or circumduction. However, despite the noticeable improvements in functional performance, the usages of systems that have considerable masses, bulky sizes or off-board actuators hold limitations in the practical perspective. It has been reported that small mass additions to the ankle can affect the natural biomechanics during gait and has large penalties in terms of the net metabolic rate [9], [10].

*This work was supported by the Bio & Medical Technology Development Program of the National Research Foundation (NRF) funded by the Korean government (MSIP) (No. NRF-2017M3A9E2063101)

S. Kim, J. Park, W. Shin and J. Kim are with the Korea Advanced Institute of Science and Technology (KAIST), Daejeon, 305701, Republic of Korea (phone: +82-42-350-5270; e-mail: jungkim@kaist.ac.kr).

D. Lee. is with the Dept. of Orthopedic Surgery at Seoul National University Hospital, Republic of Korea (e-mail: leedy@snu.ac.kr).

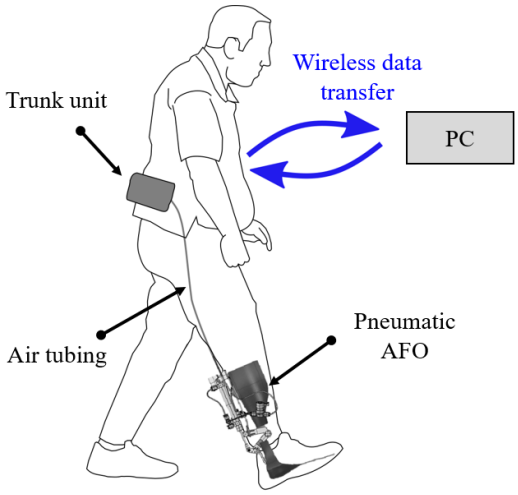

Fig. 1 System overview of the fully portable pneumatic AFO.

To minimize such counterproductive effects, a lightweight portable soft exosuit was developed with garment-like, functional textile anchors and cable-based transmissions [5], [6], [11]–[13]. Electric motors and Bowden cables were used to remotely transmit the force generated at the waist of the body to the ankle. In this way, the system was configured so that heavy mechanical and electrical components were placed closer to the trunk of the body (center of mass of the body), and therefore greatly reducing the metabolic penalty to the wearer and minimizing distortion of the natural motion.

In case of remote actuation with cable-based transmission, the tension in cables is a critical aspect that must be considered for high bandwidth force transmission, back-drivability and robot-to-user compliance [14]. High tension in cables is desirable in perspective of the control bandwidth for force transmission, however can lead to undesired resistive forces causing discomfort to the wearer. Assistive force also becomes a function of the cable position or posture of the wearer, properties of the textile anchors and structure and compliance of the human tissue that supports the anchors [14]. Therefore, complex pre-tensioning control algorithms are required.

Another widely used remote actuation method in wearable systems is using pneumatic transmission [4], [12], [15]–[19]. Pneumatic transmission has many advantages in wearable robotic applications since there is flexibility in placing pneumatic components because bending of air tubes does not significantly affect the transmission output. This allows to easily distribute the weight of the system over the body. The inherent compliance generated by the compressibility of air also allows safe user to robot interaction without additional control or elastic mechanisms. Moreover, back-drivability can be easily and effectively realized with simple valve control.

However, in order to provide sufficient assistive force/torque for wearable robotic systems, generally, large stationary air compressors with high output pressure and flowrate are required. In this study, based on our previous work on developing a high output pressure portable compressor [20], we propose a fully portable pneumatic AFO system. The flow rate of the custom compressor was optimized to provide sufficient pressure for periodic assistance of drop-foot patients with weak dorsiflexor muscles. For the design of the AFO system, to minimize the effect of additional mass attached to ankle, unnecessary and heavy components were placed at the trunk of the wearer and the AFO was simplified.

The paper is organized as follows: Section II includes the hardware design and characterization of the fully portable pneumatic AFO system and the control algorithm for drop foot assistance. Section III includes system validation by testing the proposed system on two unilateral drop foot patients. Finally, possible improvements that can be made to the system and our future work are discussed in Section IV.

II. Hardware Development

The overall system can be divided into two parts: a pneumatic AFO and a trunk unit (Fig. 1). All components with considerable mass including the custom compressor, controller, battery pack and air reservoir were included to the trunk unit. The mass distribution of the key components of the proposed system are as shown in Fig. 2-(a).

A. Hardware design of the pneumatic AFO

The main components of the pneumatic AFO are an output pneumatic cylinder, a metallic slider-crank mechanism, custom thermoplastic braces, two 2-way solenoid valves, a pressure sensor, a magnetic encoder and two custom optical type ground reaction force (GRF) sensors as shown in Fig. 3-(a).

The two 2-way solenoid valves (EC-2-12, Clippard, USA) are used to supply and discharge pressurized air to the output cylinder (SD16N75-B, Taiyo, Japan) and the pressure sensor (PSE540, SMC, Japan) is used to monitor the pressure of the output cylinder. An absolute magnetic encoder (I2A systems, Rep. of Korea) was installed to monitor the ankle flexion angle and the two custom optical GRF sensors were installed on the foot brace at the toe and heel for gait phase detection [20], [21]. The thermoplastic braces were designed so that the pneumatic AFO can be worn within the shoe and pants.

A basic slider crank mechanism was implemented to transform the linear motion of the pneumatic cylinder to rotational motion for the ankle joint. The output torque, T_{assist}, provided by the output cylinder can be calculated with the following equation,

$$F_{cyl} = P_{cyl} A_{cyl} \tag{1}$$

$$T_{assist} = F_{cyl} R \sin(\alpha + \beta) \tag{2}$$

where F_{cyl} is the force generated by the output cylinder, P_{cyl} is the pressure of the cylinder, A_{cyl} is the cross-sectional area of the cylinder, R is the moment arm and α and β are the angles

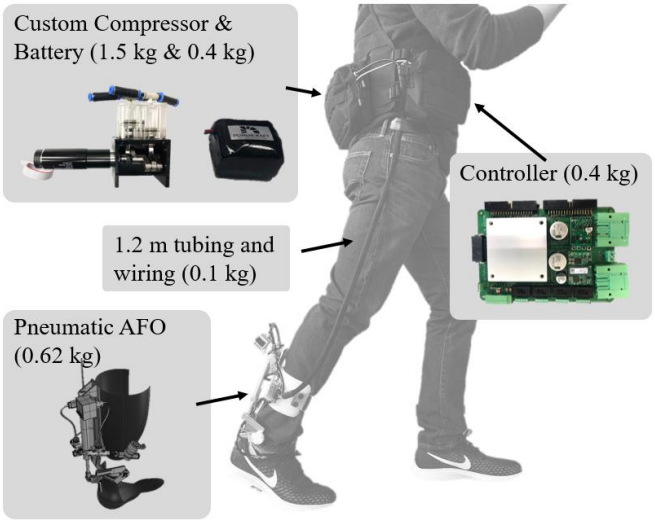

(a)

(b)

Fig. 2 (a) System overview with masses of the key components. Most of the mass is attached to the trunk of the body to minimize metabolic penalty and kinematic asymmetry. The pneumatic AFO can be worn within the pants. (b) highly modular MOLLE vest to place components on the trunk.

as shown in Fig. 3-(b). The moment arm (R) is a function of the stroke of the pneumatic cylinder (l_{cyl}). The output torque (T_{assist}), therefore, varies depending on the angle of the ankle, θ_{ank}, by 10 %. As cross-sectional area of the cylinder is proportional to assistive torque, with higher cylinder pressure the cylinder size can be reduced leading to a lighter AFO.

A. Trunk unit

The trunk unit consists a custom compressor, a controller (NI-myRIO-1900, National Instruments, USA) attached to a custom master board, an air reservoir and a 33.6 V Li-ion battery pack (33.6 V for 5.7 Ah, Powercraft, Rep. of Korea) as shown in Fig. 2-(a). On the custom master board, there are two solenoid valve drivers (EVPD-2, Clippard, USA), a buck converter to step-down the 33.6 V battery to 12 V and 24 V, a pressure sensor (ISE30A, SMC, Japan) and a DC motor driver (G2 High-Power Motor Driver 24v13, Pololu, USA) to control the custom compressor. A more detailed explanation of the custom compressor is included in the following section. The custom master board is connected to the pneumatic AFO via a 1.2 m cable. The cable was bounded together with an air tube (6 mm diameter) using braided cable sleeves. All sensor data acquired at the master board is transferred to the controller. Data is saved within the controller and can also be

transferred to a PC in real-time for monitoring via Wi-Fi. All mechanical and electrical components were distributed evenly over the trunk using a MOLLE vest (VTAC LBE Tactical Vest, 5.11 Tactical, USA) and sizable MOLLE pouches (Fig. 2-(b)). The high modularity and compatibility of pouches allowed varying the locations of each component and distributing the masses as desired.

B. Custom pneumatic compressor

There are a few portable pneumatic energy sources that have been introduced throughout the literature for wearable robotic applications [22]–[31]. There are sources that rely on direct chemical reactions [22], [23], [25]–[28], [32], sources that use compressed gases or liquids in a vessel or sources that mechanically compress ambient air from the atmosphere [4], [7]. All sources carry distinct advantages and innovative results have been reported showing great potentials for wearable applications. In this study, based on our previous work [33], we implemented a high pressure custom dual piston crank compressor that is powered by a DC motor. It is a safe (hazard free), clean (no chemical byproducts) and robust method to continuously generate high pressure air based on electric power which makes it suitable for daily applications. In this study, we improved the previously developed compressor by optimizing the rate of compression to the rate of air consumption required to power the pneumatic AFO.

The design requirement of the custom compressor was set to power the unilateral pneumatic AFO for drop foot correction. Drop foot patients commonly have difficulty in foot clearance during the swing phase of the gait cycle (GC), thus only requiring assistive torque during this phase. The assistive torque required for full dorsiflexion for patients with spasticity or muscle weakness was set to 10 Nm. With (1) and (2), the minimum pressure required to generate 10 Nm, considering the variation in the moment arm (R), is 550 kPa. We have selected a functional frequency of 1 Hz based on the average stride of adults [34].

With these requirements, the main goal was to accumulate sufficient amount of pressurized air in the reservoir during the stance phase (when no assistive torque is required), then transmitting the accumulated pressurized air to the output cylinder by controlling the supply valve (V_{supply}) and discharge valve ($V_{discharge}$) during the swing phase. Therefore, sufficient amount of air must be accumulated during the stance phase which is generally 60 % of the GC or approximately 0.6 s [34]. Therefore, considering the output cylinder volume of the AFO, the theoretical rate of compression must meet 550 kPa at a rate of 15.1 mL/s to accumulate enough pressurized air during the stance phase.

We have utilized the identical dual piston crank parameters as introduced in [33], but have replaced the DC motor that powers the compressor. Depending on the rotational velocity of the DC motor, the rate of compression (Q) can be changed. The maximum flow rate to generate 550 kPa of pressurized air can be calculated as,

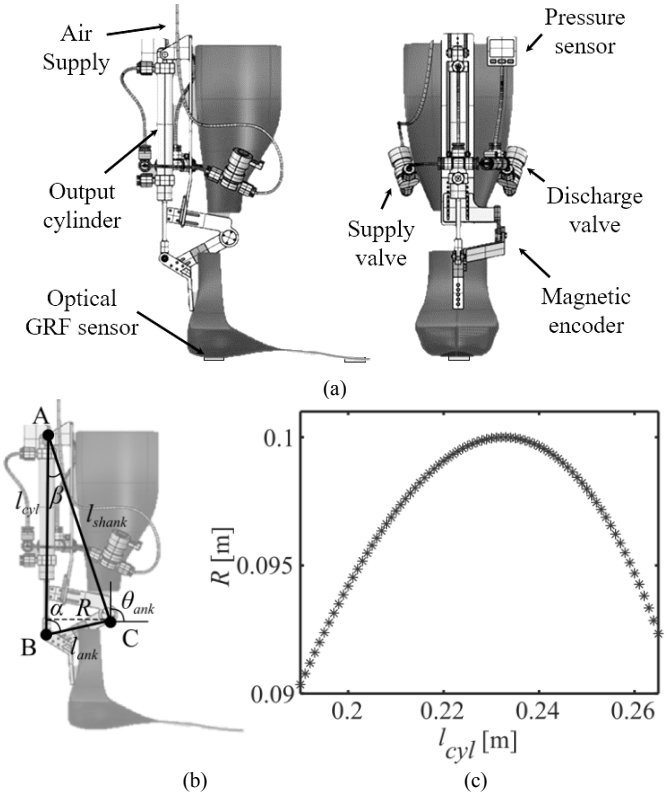

Fig. 3 (a) Overview of the active ankle foot orthosis (AFO). Two 2-way solenoid valves are used to control the supply and discharge of pressurized air to the output cylinder. (b) Kinematic model of the slider crank mechanism used to transfer the linear motion of the output cylinder to rotational motion and (c) the moment arm, R, with respect to the stroke of the output cylinder (l_{cyl}). The stroke of the output cylinder is 0.075 m.

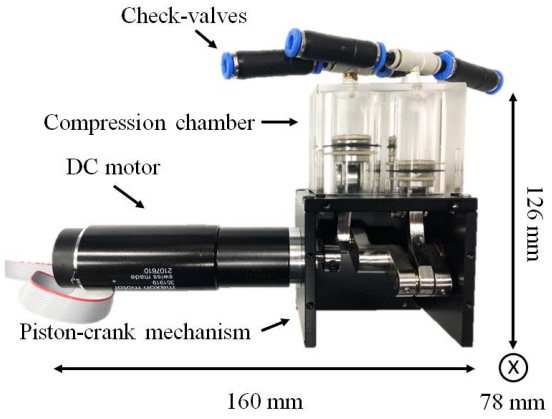

Fig. 4 Dual crank compressor to power the proposed AFO. The custom compressor is 1.5 kg.

$$Q = 1.91\ V_c\ (2K) \tag{3}$$

where V_c is the volume that is compressed during a single compression cycle (volume at TDC) and K is the nominal number of rotations per second of the DC motor. 1.91 is the ratio between the maximum pressure, 1050 kPa, and the required pressure, 550 kPa. 2 is a factor due to the double piston. A DC motor (RE35, Maxon Motor, Switzerland) with a nominal velocity that meets the requirement to compress 15.5 mL/s of 550 kPa of pressurized was selected. The experimental evaluation of the compressor is given in the

following section.

C. Control strategy

Custom optical GRF sensors are used to detect different phases during the GC. The GC is divided into four phases (heel strike, foot flat, heel off and toe off) based on the activation of the sensors. The sensors provide a continuous analog output voltage; therefore, the activation is determined based on a user-defined threshold level.

During the entire GC, the custom compressor is activated at nominal ratings. When stance phase of the GC is detected, V_{supply} is closed blocking the transfer of pressurized air from the reservoir and air tubing to the output cylinder. This leads to the accumulation of pressurized air in the reservoir and air tubing up to the point of the V_{supply} (Fig. 5–(a)). Instantaneously, $V_{discharge}$ is opened so that air within the output cylinder can freely move back and forth between the environment (atmosphere). This allows free movement of the ankle during the stance phase. Generally, the weight of the body allows drop-foot patients to achieve normal ankle kinematics.

During the swing phase, as assistive torque is required by the proposed AFO, the accumulated pressurized air is transferred to the output cylinder by controlling V_{supply} and $V_{discharge}$ in an on-off manner (Fig. 5–(b)). The swing phase starts with the toe off state and ends with heel strike.

D. System validation

The proposed system was tested to validate if sufficient amount of pressurized air can be accumulated during the stance phase of the GC. The experimental setup is as shown in Fig. 5. The DC motor of the custom compressor was activated at nominal ratings and a continuous feedforward 1.67 Hz square voltage waveform was applied to the two solenoid valves. The square voltage inputs were inverted for V_{supply} and $V_{discharge}$. The excitation frequency of the square waves was selected considering that the stance phase of the GC is approximately 0.6 s during overground walking [34]. This excitation is equivalent to the condition of a 0.6 s stance phase followed by a 0.6 s swing phase. Fig. 6-(a) shows the resulting reservoir and output cylinder pressure. Since the reservoir of the pneumatic circuit was initially empty, it takes approximately 8 s to generate full desired pressure in the output cylinder. During this period, as we optimized the compressor to generate 550 kPa at a rate of 15.1 mL/s (to achieve 10 Nm), however, not as much is being consumed (or exhausted) at the output cylinder, air accumulates within the reservoir. However, after 8 s, as the rate of compression and the rate of air consumption becomes identical, the output pressure saturates at approximately 550 kPa. The saturated maximum pressure of the output cylinder can be reduced depending on the required output torque by activating the DC motor of the custom compressor at slower rotational velocities.

The back-drivability of the system was also tested. As aforementioned, free movement is provided during the stance phase (0~60% of the GC). The pressure of the output cylinder

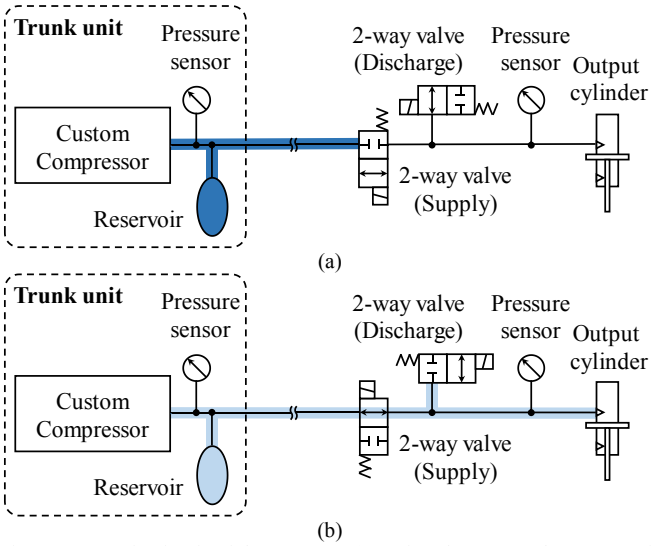

Fig. 5 Pneumatic circuit of the system. (a) During the stance phase, V_{supply} is closed and the $V_{discharge}$ is opened. This allows free movement of the ankle and accumulation of air in the reservoir. (b) During the swing phase, the accumulated air is supplied to the output cylinder to assist dorsiflexion. 1.2m air tubing between the trunk unit and pneumatic AFO.

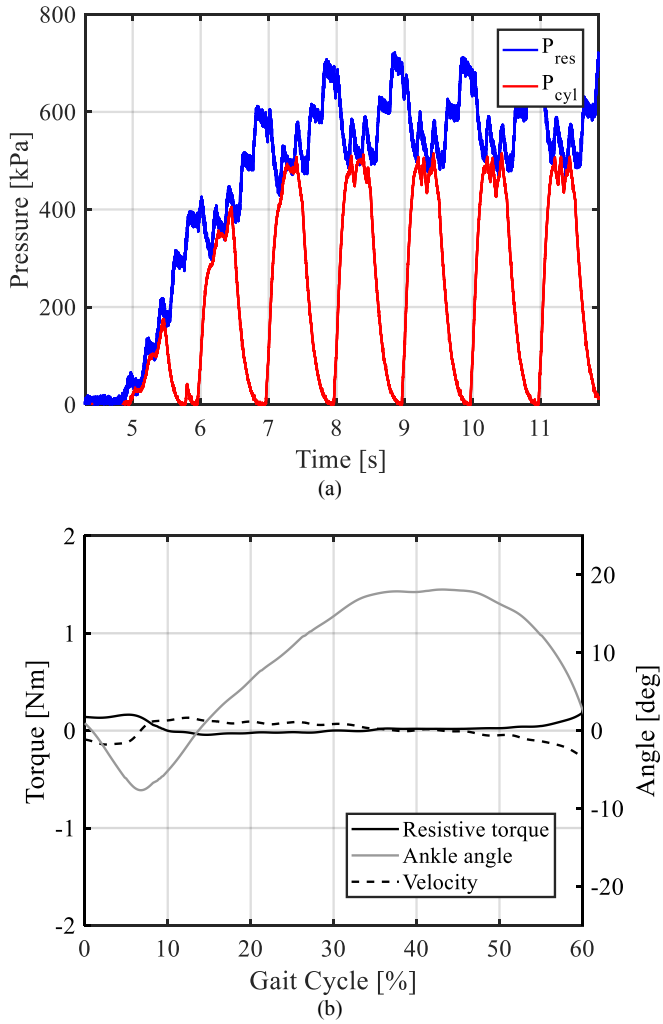

Fig. 6 (a) Reservoir and output cylinder pressure when custom compressor was activated with nominal ratings and a square wave form with a frequency of 1.67 Hz was fed to the two 2-way solenoid valves. (b) Resistive torque during a full GC. Free movement is only allowed during the stance phase; however, the full GC was tested.

was measured during this period while V_{supply} is closed and $V_{discharge}$ was opened. With the pressure of the output cylinder, the resistive torque applied due to the ankle can be estimated using (2). The resistive torque generated from the AFO during this period is as shown in Fig. 6-(b). The generated resistive torque was highly correlated to the velocity profile, namely, due to viscous friction. An average resistive torque of 0.03±0.06 Nm was generated during 0~60 % of the GC. The peak resistive torque during the stance phase was 0.18 Nm. Note that the peak resistive torque during the swing phase is approximately 0.81 Nm and the average resistive torque is 0.04±0.21 Nm, however, is not considered in this study as assistance is applied during this phase.

III. Unilateral Drop Foot Patient Walking Test

A. Experimental setup

To validate the feasibility of the proposed system in assisting hemiplegic drop foot gait, a test was conducted on two unilateral drop foot patients. Both patients were able to walk independently for 10 min without rest. The experiment focused on evaluating the effect of the proposed system in assisting foot dorsiflexion while not disturbing natural gait during the stance phase. Detailed demographic information of the patients who have participated in the experiment is reported in Table 1.

Patients were asked to walk along a 9-m track equipped with 12 motion capture cameras (Motion Analysis, USA). Data was collected with a sampling rate of 120 Hz. The three-dimensional accuracy of the system is less than 0.6 (standard deviation 0.2-0.3) mm. Intra- and inter-session repeatability of motion analysis was reliable (intra-class correlation coefficients for lower extremity motion, 0.93-0.99). The experimental setup is as shown in Fig. 7.

For three different conditions: walking 1) with common commercial shoes, 2) with the proposed AFO unpowered (AFO_{OFF}) and 3) with the proposed AFO powered (AFO_{ON}). For the two AFO conditions, identical shoes with condition 1) was used. We use the common commercial shoe as the baseline, instead of the barefooted condition, to minimize the effect of the error in optical marker attachment.

For each condition, the patients were asked to walk ten laps of the 9-m track. For the AFO_{OFF} condition, the compressor was not powered and the discharge valve was opened to provide free ankle movement. For the AFO_{ON} condition, the velocity of the DC motor for the custom compressor was adjusted for each participant so that positive ankle dorsiflexion angle was achieved during the swing phase (60~100% GC). Approximately, 0˚ ankle dorsiflexion angle during the swing phase can prevent major falls during gait [5].

All walking conditions were self-paced and a 10 min resting period was provided between each condition. All walking trials were supervised by a licensed physical therapist (PT). The average of five representative strides was used in the analysis. Joint kinematics was calculated using Visual 3D software (C-Motion Inc., USA). The experimental protocol was approved by the International Review Board of Seoul National University Hospital (SNUH). Written informed consent and assent were obtained from each participant.

Table 1 Demographic information of the two foot drop patients

Patient No.	Age	Gender	Weight	Height	Paretic side	Chronicity
	yr		kg	cm		yr
S01	63	Male	68.9	173.4	Left	8
S02	61	Female	64.4	152.0	Left	1

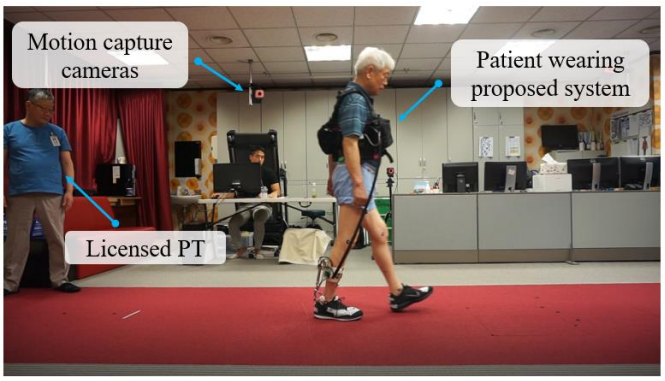

Fig. 7 Experimental setup for the patient walking test.

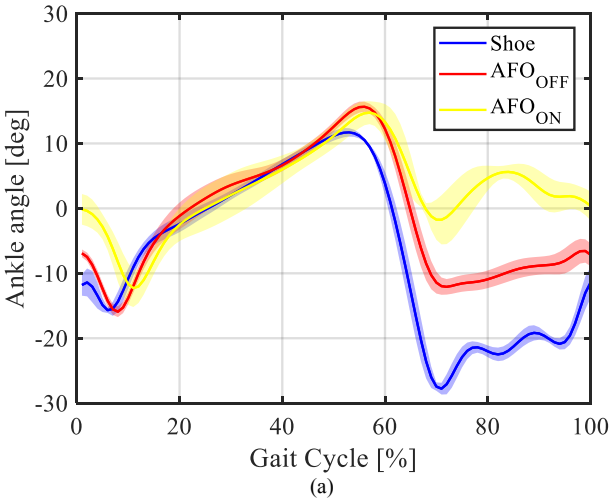

(a)

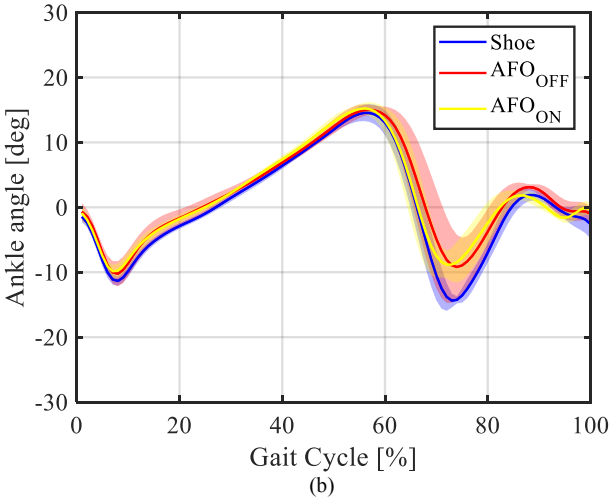

(b)

Fig. 8 Ankle flexion angle in the sagittal plane of S01. a) the ankle with drop foot and b) the unaffected ankle. The shaded regions show the standard deviation of the five representative walking trails. Positive values are the dorsiflexion angle and negative values are the plantar flexion values.

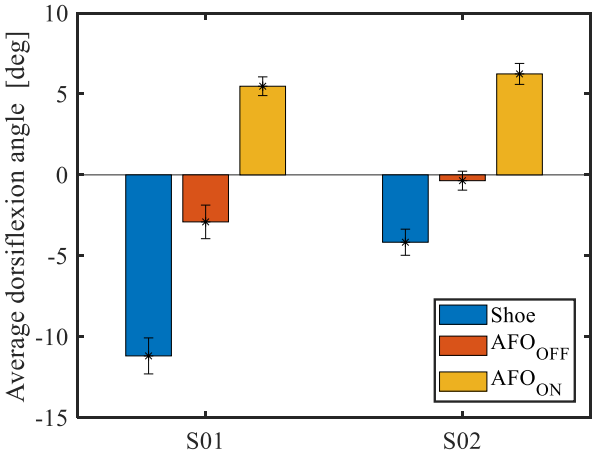

Fig. 9 Average dorsiflexion angle for five steps during 70~100% of the GC with standard deviations.

Table 2 Mean and standard deviation of the ankle dorsiflexion angle during 70~100% GC

Cond.	Shoe	AFO_{OFF}	AFO_{ON}
S01	-11.2±1.1	-2.9±1.0	5.5±0.6
S02	-4.2±0.8	-0.6±0.6	6.2±0.6

B. Results

In this study, we focused on the immediate improvements in the ankle kinematics with DF assistance, not on long-term changes that may arise from sustained usage. Ankle kinematic data in the sagittal plane for five steps of a representative patients is as shown in Fig. 8. Ankle flexion angle is defined using the coordinate system as shown in Fig. 3-(b). Positive values are for ankle dorsiflexion and negative for plantar flexion. The average plantarflexion angle during 70~100% of the GC for the three conditions (shoe, AFO_{OFF} and AFO_{ON}) is shown in Fig. 9. The mean and standard deviations are shown in Table 2. An average 13.6° improvement in peak dorsiflexion was achieved between the shoe and AFO_{ON} condition. Dorsiflexion angle also improved by an average of 6.0° for the AFO_{OFF} condition. This was due to viscous friction of the output cylinder during the swing phase.

IV. Discussion and Conclusion

Previously, an fully portable pneumatic AFO system powered by a compressed CO_2 vessel has been developed and analyzed [4][7]. The system was the first fully portable pneumatic system and promising clinical results have been reported showing the advantages of pneumatic transmission throughout the literature. The use of high-pressure fluid vessels, however, have several limitations. Due to the limited duration of operation, vessel replacements or increased size and weight of the vessels is required which can be undesirable for wearable applications. Furthermore, additional pressure regulation components are required, to modulate the high supply pressure to pressure levels that can be used to power the AFO, leading to bulky system size and weight [4]. The blockage of air tubing due to freezing from endothermic expansion of highly pressurized gases must also be considered since gait assistive devices require repeated continuous high flow of pressurized fluids.

In this study, we introduced the concept of applying a compressor that mechanically compresses ambient air using an electric motor. This is a safe (no major safety hazards) and clean (no chemical byproducts) method to generate compressed air. The output pressure levels and compression rate of the compressor can be designed and optimized according to the power requirements of the wearable device (another example is shown in [18], [19]). The use of electrical power (Li-ion battery pack) to produce pressurized air is an advantage as most robotic systems require electrical power for sensors and controllers, therefore not requiring an additional power source.

The current mechanical output of the custom compressor, however, is approximately 8W which is relatively low compared to most previously introduced AFO systems. In the current version of the compressor, we have mainly focused on producing large maximum pressure, approximately 1050kPa, to reduce the output cylinder size used in the AFO (the cross-sectional area of the pneumatic cylinder can be reduced). As shown in [33], starting from 800 kPa, considerable air leakage between the piston head and compression cylinder was observed. In our future work, we will lower the compression ratio while increasing the compression rate so that we can achieve the same output but with less leakage. We will also improve the sealing between the piston head and compression cylinder of the compressor.

In terms of the AFO system, we have not considered the accurate timing of assistance and have only tested the system with a basic ON/OFF controller which is activated based on a user-defined GRF detection algorithm. This led to the hindrance during ankle push off state. In our future work, we will systematically investigate the response time of the transmission system and the effect of gait phase detection time, to improve the timing of assistance.

References

[1] G. Anderson and J. Horvath, "The growing burden of chronic disease in America," *Public Health Rep.*, vol. 119, no. 3, pp. 263–270, 2004.

[2] M. Ory, M. K. Hoffman, M. Hawkins, B. Sanner, and R. Mockenhaupt, "Challenging aging stereotypes: Strategies for creating a more active society," *Am. J. Prev. Med.*, vol. 25, no. 3 SUPPL. 2, pp. 164–171, 2003.

[3] J. A. Blaya and H. Herr, "Adaptive Control of a Variable-Impedance Ankle-Foot Orthosis to Assist Drop-Foot Gait," *IEEE Trans. Neural Syst. Rehabil. Eng.*, vol. 12, no. 1, pp. 24–31, 2004.

[4] K. A. Shorter, G. F. Kogler, E. Loth, W. K. Durfee, and E. T. Hsiao-Wecksler, "A portable powered ankle-foot orthosis for rehabilitation," *J. Rehabil. Res. Dev.*, vol. 48, no. 4, pp. 459–472, 2011.

[5] L. N. Awad *et al.*, "A soft robotic exosuit improves walking in patients after stroke," *Sci. Transl. Med.*, vol. 9, no. 400, pp. 1–13, 2017.

[6] L. N. Awad *et al.*, "Reducing Circumduction and Hip Hiking During Hemiparetic Walking Through Targeted Assistance of the

Paretic Limb Using a Soft Robotic Exosuit," *Am. J. Phys. Med. Rehabil.*, vol. 96, no. 10, pp. S157–S164, 2017.
[7] M. K. Boes *et al.*, "Six-Minute Walk Test Performance in Persons With Multiple Sclerosis While Using Passive or Powered Ankle-Foot Orthoses," *Arch. Phys. Med. Rehabil.*, vol. 99, no. 3, pp. 484–490, 2018.
[8] J. Kwon, J. Park, S. Ku, Y. Jeong, N. Paik, and Y. Park, "A Soft Wearable Robotic Orthosis for Ankle Rehabilitation of Post-Stroke Patients," pp. 2–8, 2019.
[9] R. C. Browning, J. R. Modica, R. Kram, and A. Goswami, "The effects of adding mass to the legs on the energetics and biomechanics of walking," *Med. Sci. Sport. Exerc.*, vol. 39, no. 3, pp. 515–525, 2007.
[10] R. L. Waters and S. Mulroy, "The energy expenditure of normal and pathologic gait," *Gait Posture*, vol. 9, pp. 207–231, 1999.
[11] L. M. Mooney, E. J. Rouse, and H. M. Herr, "Autonomous exoskeleton reduces metabolic cost of human walking during load carriage," *J. Neuroeng. Rehabil.*, vol. 11, no. 1, p. 80, 2014.
[12] P. Malcolm, W. Derave, S. Galle, and D. De Clercq, "A Simple Exoskeleton That Assists Plantarflexion Can Reduce the Metabolic Cost of Human Walking," *PLoS One*, vol. 8, no. 2, pp. 1–7, 2013.
[13] Z. F. Lerner *et al.*, "An untethered ankle exoskeleton improves walking economy in a pilot study of individuals with cerebral palsy," *IEEE Trans. Neural Syst. Rehabil. Eng.*, vol. 26, no. 10, pp. 1985–1993, 2018.
[14] A. T. Asbeck, R. J. Dyer, A. F. Larusson, and C. J. Walsh, "Biologically-inspired soft exosuit," *IEEE Int. Conf. Rehabil. Robot.*, 2013.
[15] P. Malcolm, P. Fiers, V. Segers, I. Van Caekenberghe, M. Lenoir, and D. De Clercq, "Experimental study on the role of the ankle push off in the walk-to-run transition by means of a powered ankle-foot-exoskeleton," *Gait Posture*, vol. 30, no. 3, pp. 322–327, 2009.
[16] D. P. Ferris, K. E. Gordon, G. S. Sawicki, and A. Peethambaran, "An improved powered ankle-foot orthosis using proportional myoelectric control," *Gait Posture*, vol. 23, no. 4, pp. 425–428, 2006.
[17] P. C. Kao, C. L. Lewis, and D. P. Ferris, "Invariant ankle moment patterns when walking with and without a robotic ankle exoskeleton," *J. Biomech.*, vol. 43, no. 2, pp. 203–209, 2010.
[18] U. Heo, S. J. Kim, and J. Kim, "Backdrivable and Fully-Portable Pneumatic Back Support Exoskeleton for Lifting Assistance," *IEEE Robot. Autom. Lett.*, vol. 5, no. 2, pp. 1–1, 2020.
[19] J. Park, J. Choi, S. J. Kim, K. Seo, and J. Kim, "Design of an Inflatable Wrinkle Actuator with Fast Inflation / Deflation Responses for Wearable Suits," vol. 3766, no. c, pp. 1–7, 2020.
[20] S. J. Kim, G. M. Gu, Y. Na, J. Park, Y. Kim, and J. Kim, "Wireless Ground Reaction Force Sensing System Using a Mechanically Decoupled Two-Dimensional Force Sensor," *IEEE/ASME Trans. Mechatronics*, vol. 4435, no. c, pp. 1–1, 2019.
[21] J. Park, S. J. Kim, Y. Na, Y. Kim, and J. Kim, "Development of a Bendable Outsole Biaxial Ground Reaction Force Measurement System," 2019.
[22] M. Goldfarb, E. J. Barth, M. A. Gogola, and J. A. Wehrmeyer, "Design and energetic characterization of a liquid-propellant-powered actuator for self-powered robots," *IEEE/ASME Trans. Mechatronics*, vol. 8, no. 2, pp. 254–262, 2003.
[23] Y. Hong, S. Member, K. Kim, K. Kim, and S. Kim, "A novel pneumatic generator with pressure-feedback mechanism for self-injection of hydrogen peroxide," *IEEE Trans. Mechatronics*, vol. 4435, no. c, pp. 1–11, 2017.
[24] T. G. McGee and J. W. Raade, "Monopropellant-driven free piston hydraulic pump for mobile robotic systems," *J. Dyn. Syst. Meas. Control*, vol. 126, no. March 2004, pp. 75–81, 2017.
[25] H. Wu, A. Kitagawa, H. Tsukagoshi, and C. Liu, "Development of a novel pneumatic power assisted lower limb for outdoor walking by the use of a portable pneumatic power source," *Proc. IEEE Int. Conf. Control Appl.*, no. October, pp. 1291–1296, 2007.
[26] M. Gogola, E. J. Barth, and M. Goldfarb, "Monopropellant powered actuators for use in autonomous human-scaled robotics," *Proc. - IEEE Int. Conf. Robot. Autom.*, vol. 3, no. May, pp. 2357–2362, 2002.
[27] K. Kim, Y. Hong, K. Kim, and S. Kim, "Design of a compact pneumatic power generator with a self-regulating mechanism for mobile application," *IEEE Trans. Mechatronics*, vol. 4435, no. c, pp. 1–9, 2017.
[28] A. Kitagawa, H. Wu, H. Tsukagoshi, and S.-H. Park, "Development of a portable pneumatic power source using phase transition at the triple point," *Trans. Japan Fluid Power Syst. Soc.*, vol. 36, pp. 158–164, 2005.
[29] K. B. Fite and M. Goldfarb, "Design and rnergetic characterization of a proportional-injector monopropellant-powered actuator," *IEEE Trans. Mechatronics*, vol. 11, no. 2, pp. 196–204, 2006.
[30] M. Okui, Y. Nagura, Y. Yamada, and T. Nakamura, "Hybrid pneumatic source based on evaluation of air compression methods for portability," *IEEE Robot. Autom. Lett.*, vol. 3, no. 2, pp. 819–826, 2018.
[31] M. Wehner *et al.*, "Pneumatic energy sources for autonomous and wearable soft robotics," *Soft Robot.*, vol. 2, no. 00, pp. 1–12, 2014.
[32] R. F. Shepherd *et al.*, "Using explosions to power a soft robot," *Angew. Chemie Int. Ed.*, vol. 52, pp. 2892–2896, 2013.
[33] S. J. Kim, H. Chang, J. Park, and J. Kim, "Design of a Portable Pneumatic Power Source with High Output Pressure for Wearable Robotic Applications," *IEEE Robot. Autom. Lett.*, vol. 3, no. 4, pp. 4351–4358, 2018.
[34] H. Stolze *et al.*, "Gait analysis during treadmill and overground locomotion in children and adults," *Electroencephalogr. Clin. Neurophysiol. - Electromyogr. Mot. Control*, vol. 105, no. 6, pp. 490–497, 1997.